In silico Derivation of a Reduced Kinetic Model for Stationary or Oscillating Glycolysis in *Escherichia coli* Bacterium

doi: 10.15255/CABEQ.2014.2002

G. Maria*
Department of Chemical & Biochemical Engineering
University Politehnica of Bucharest, Romania

Original scientific paper
Received: February 2, 2014
Accepted: September 4, 2014

Modelling bacteria glycolysis is a classical subject but still of high interest. Glycolysis, together with the phosphotransferase (PTS)-system for glucose transport into the cell, the pentose-phosphate pathway (PPP), and tricarboxylic acid cycle (TCA) characterize the central carbon metabolism. Such a model usually serves as the foundation for developing modular simulation platforms used for consistent analysis of the control / regulation of target metabolite synthesis. The present study is focused on analyzing the advantage and limitations of using a simplified but versatile 'core' model of mTRM) of glycolysis when incomplete experimental information is available. Exemplification is made for a reduced glycolysis model from literature for *Escherichia coli* cells, by performing a few modifications (17 identifiable parameters) to increase its agreement with simulated data generated by using an extended model (127 parameters) over a large operating domain of an experimental bioreactor. With the expense of ca. 8–13 % increase in the relative model error vs. extended simulation models, derivation of reduced kinetic structures to describe some parts of the core metabolism is worth the associated identification effort, due to the considerable reduction in model parameterization (e.g. 17 parameters in mTRM vs. 127 in the extendedChassM model of Chassagnole et al.), while preserving a fair adequacy over a wide experimental domain generated in-silico by using the valuable extended ChassM. The reduced model flexibility is tested by reproducing stationary or oscillatory glycolysis conditions. The reduced mTRM model includes enough information to reproduce not only the cell energy-related potential through the total A(MDT)P level, but also the role played by ATP/ADP ratio as a glycolysis driving force. The model can also reproduce the oscillatory behaviour occurrence conditions, as well as situations when homeostatic conditions are not fulfilled.

Key words:
dynamic model, glycolysis, *Escherichia coli*, reduced model identification, oscillations

Introduction

Modelling the central carbon metabolism, and particularly the glycolysis pathway in bacteria is one of the essential bioengineering / bioinformatics topics as long as these models, completed by the –omics data, are considered as a 'core' part of any systematic and structured analysis of the cell metabolism with immediate practical applications (such as target metabolite synthesis optimization, *in silico* reprogramming of the cell metabolism and design of new micro-organisms, bioreactor / bioprocess optimization[1–3]). Such representations are able to simulate, in a consistent and accurate way and at a certain degree of detail, the kinetics of a large number of cell biosyntheses and genetic circuits controlling the cell adaptation to environmental changes.

However, to cope with the astronomic complexity of cellular processes, of low observability, involving O(10^3–10^4) number state variables (species conc.), O(10^3) gene expression transcription factors TF, and O(10^4–10^5) reactions, versatile models of 'building-blocks' like modular constructions including individual and lumped species and reactions have been developed over decades. These models are based on the observation that the gene network is sparsely interconnected (e.g. one gene interacts with maximum other 23–25[4,5]), and the cellular syntheses regulatory network is a modular structure (hierarchically organised) with a certain repeatability of gene expression control.[6] Such an approach allows reducing the model complexity by relating the cell response to stimuli in response to only a few metabolic reactions and regulatory loops instead of the response of thousands of regulatory circuits in gene expression over a complex metabolic pathway.[7,8] Thus, the model identification becomes a problem of simultaneous model structure and parameter identification.[7,9,10] By using the concepts of '*reverse engineering*' and '*integrative un-*

*Corresponding author: P.O. 35-107 Bucharest, Romania;
Tel: 40 744 830308; Email: gmaria99m@hotmail.com

derstanding',[1,11] such a rule seeks reduction of the identification effort by disassembling the cell system into parts (functional modules), which can be individually studied and characterized, and then, following an appropriate linking algorithm, the whole metabolic pathway and the afferent genetic regulatory circuit are recreated for reproducing the real system. Application of such advanced lumping techniques increases model estimability by reducing the number of considered reactions and species, by keeping the most influential terms related to a target synthesis.

The assumed model reduction cost is related to the loss of information on certain species and reactions, a loss in model generality, prediction capabilities, physical meaning of some rate constants, and alteration of some systemic properties (stability, multiplicity, sensitivity, regulatory characteristics). Such model reduction drawbacks are compensated by the model's simplicity, computer tractability, easier rate constant identification from usually incomplete structured data sets, interpretable representation of the cell complexity (sometimes in an analytic computational way), and quicker *in silico* cell design possibilities.

For linear kinetic models there are standard procedures for exact or approximate model reduction based on the analysis of system invariants, stoichiometric matrix properties, and the number of independent species and reactions leading to determine the link matrix between the extended and reduced models.[12] However, for extended nonlinear kinetic models (such as the case of cell metabolic processes), there is no general reduction rule to be applied. For such situations, model quality tests, sensitivity analysis of model outputs vs. parameters and species concentrations, principal component, and other algorithms to find the redundant part of the model should be applied.[13–15]

Due to the enormous complexity of metabolic processes, and differences between enzyme Michaelis-Menten rate constants determined from separate *in-vitro* experiments and those determined from *in-vivo* metabolic data, the extended model rate constants are either imported from other separate modelling studies, or identified, or eventually eliminated based on available (usually incomplete) kinetic data sets.[1,16] Recent advances in experimental techniques, such as the time-series micro-array data with a sampling frequency of seconds to minutes[17,18] will create the possibility to continuously expand and improve such metabolic dynamic models.

In any alternative – reduced or extended, a 'core' model of the central carbon metabolism, completed with extensions describing target metabolite syntheses, and involved genetic control circuits can achieve a satisfactory trade-off between model simplicity and predictive quality, being able to simulate the organism behaviour under specified conditions. Various applications are reported, such as optimization of synthesis of amino-acids (AA),[19–22] ethanol,[23–24] succinate,[25] lactate,[26] or other metabolites in mutant cells[27,28]. Deterministic simulation platforms allow *in silico* design of modified cells with desirable gene circuits and 'motifs' of practical applications in the biosynthesis industry, environmental engineering, and medicine.

A large number of bacteria glycolysis models, of a reduced or extended form depending on the available information and utilization purpose, have been proposed over decades. Among them are those developed for *E. coli* glycolysis by:

– Selkov[29] (5 species, 5 reactions)

– Termonia and Ross[30,31] (TRM, 9 species, 7 reactions, 19 parameters)

– *Hatzimanikatis & Wang*[32] (6 species, 9 reactions)

– Bier et al.[33] (7 species, 9 reactions, 15 parameters)

– Buchholz et al.[34] (3 species, 5 reactions, 24 parameters)

– Chassagnole et al.[16] (ChassM, 48 reactions, 18 species, 127 parameters)

– Westermark & Lansner[35] (pancreatic cells; 6 species, 6 reactions)

– Degenring et al.[14] (10 species, 22 reactions, 123 parameters)

– Ceric & Kurtanjek[36] (10 species, 24 reactions)

– Costa et al.[15] (25 species, 30 reactions, 116 parameters)

– Usuda et al.[21] (52 reactions, 23 gene expressions, 30 species)

– Kadir et al.[28] (24 species, 30 reactions, more than 150 parameters).

A significant number of models have been translated in the SBML, PYSCES or other specific programming languages, being on-line available on public simulation platforms (e.g. JWS of Olivier & Snoep[37]; Laiterä[38]).

Extensions of such glycolysis / central metabolism models can be performed accordingly to a particular interest in detailing a certain biosynthesis, by preserving the optimised regulatory properties of the 'core' model)[6,39–43] under variable volume and isotonic constraints.[7,9,10,43]

However, when modelling the kinetics of a target metabolite synthesis, it is questionable at what degree of detail the central carbon metabolism must be represented, that is glycolysis, PPP, PTS-system, TCA cycle, AA-synthsis, nucleotide metabolism,

synthesis of lipid precursors, and others (see the complete list of central metabolism reactions of *E. coli* in Ecocyc, or KEGG data-bases[16,44]). Obviously, a detailed representation of the essential cell processes better reflects the cell requirements, and the way of using the substrate from the environment together with the control of key syntheses. However, a too detailed 'core' model might increase with orders of magnitude the number of rate constants necessary to be estimated concomitantly with those of the target metabolite pathways from a quite limited amount of experimental information. Besides, complicated models of the central metabolism do not necessarily add essential information of interest for the target process modification, but might unnecessarily increase the experimental effort to identify the model parameters, and complicate further engineering computational steps for bioprocess characterization, design, optimization, and control.

One of the most valuable representations of the central carbon metabolism in *E. coli* is the Chassagnole et al.[16] model (ChassM, 48 reactions, 18 species, 127 parameters, see reaction scheme of Fig. 1-left) able to accurately reproduce the PTS-system, glycolysis, PPP, and storage material dynamics under stationary or perturbed conditions, with a model average relative error of ca. 25 % (but up to 100 % for parts of some species recovering trajectories). Being quite complex, and with a wide range of time constants of reactions (from 0.29 ms to 85 s), some authors underlined the low significance of some model terms under common environmental conditions.[15] In spite of that, ChassM remains one of the most refereed models for *E. coli* cell central metabolism simulations, being implemented on the online JWS platform.[37]

Currently, there is a collection of available reduced representations of glycolysis, including simulations of the occurrence of glycolytic oscillations, which deserve to be used for developing simplified *E. coli* metabolism models. Such a model is that of Termonia and Ross[30,31] (TRM; 9 species, 7 reactions, 19 parameters, see reaction scheme of Fig. 1-right) able to fairly simulate the cell glycolysis under steady state, oscillatory, or transient conditions according to the defined glucose input flux and total A(MDT)P cell energy resources.

The aim of this paper is to extend a comparative analysis of these two valuable models (ChassM and TRM) used for representing the glycolysis in *Escherichia coli* cells, by proposing a few completions of the reduced TRM (leading to mTRM model of 17 identifiable parameters; it is well known that reduced models lead to increased identifiability vs. data [56]) to better fit the extended ChassM model predictions over a broader bioprocess operating domain than those experimentally investigated, under both stationary and dynamic conditions.

In such a manner, at the expense of an inherent reduction in model adequacy of ca. 10 %, the gain in simplicity offered by the mTRM reduced representation, might be useful for developing simplified models of some metabolic pathways of *E. coli,* by preserving the essential features of the glycolysis process. The obtained reduced model flexibility is tested by reproducing / predicting stationary or oscillatory glycolysis conditions in the bioreactor.

Glycolysis simulation with the extended ChassM

The kinetic model proposed by Chassagnole et al.[16] (ChassM) used to simulate the central carbon metabolism in *E. coli* is quite complex and includes 48 reactions, 18 species, and 127 parameters (see reaction scheme of Fig. 1-left; rate expressions are not displayed here). The rate constants are estimated from dynamic data concerning the external glucose (GLC), and eight intra-cellular metabolite concentrations (G6P, F6P, FDP, GAP, PEP, PYR, G1P, 6PG, see notations in Fig. 1) recorded from experiments using a continuous bioreactor after applying a "pulse"-like perturbation in the glucose feeding concentration. The nominal conditions of the bioreactor from Table 1 have been adjusted to match the hydrodynamic residence time (F_L/V_L) with the culture dilution constant and the intracellular content dilution rate (D). In the bioreactor operation practice, the cell culture dilution rate (equal to the logarithmic average cell growth rate) is ranged to equal the hydrodynamic residence time to avoid the biomass washout.[55] The model initial parameter guess is taken from literature information.

Due to ChassM's high complexity, most of the enzymatic rate expressions are imported from literature, being sometimes simplified according to the acquired experimental information. Some reactions of the nonoxidative part of PPP (that is Ru5P, R5PI, TKa, TKb, TA, see Fig. 1) are assumed to reach near-equilibrium conditions, while the gene expression control is not explicitly included in the model. In addition, the mass balance describing the dynamics of nucleotide [A(MDT)P] species (that is the driving force of the glycolytic pathway, and a measure of the total cellular energy dynamics), as well as the evolution of NADH/NAD^+ and NADPH/$NADP^+$ co-factors are not included in ChassM, but recorded data are used instead during simulations thus limiting the model's predictive power over an extended operating domain.

Even if the large number of ChassM rate constants are estimated from using quite reduced experimental information (that is the kinetic data set recorded for the feeding solution of $[GLC]_{feed}$= 110.96

mmol L^{-1}), the resulting model adequacy is quite good (ca. 25 % average relative error), even if some species trajectories (FDP, PYR) reported much larger bias vs. experimental data (ca. 100 % relative error) over some parts of the transient regime. The PFK-ASE and PK-ASE are included in the rate constants, but their role as oscillation "nodes" for the coupled F6P → FDP and PEP → PYR reactions is not explicitly studied in the original paper. In principle, ChassM can describe the dynamic behavior of metabolites in the metabolic networks including the central metabolism pathway, as well as the intracellular metabolite oscillations observed experimentally.[45]

A typical simulation of the *E. coli* cell response to an applied pulse in the glucose concentration in a steady-state culture, from the stationary level of $[GLC]_s$ = 0.055 mmol L^{-1} to [GLC] = 2 mmol L^{-1} at time t = 0 is plotted in Fig. 2 under nominal operating conditions of Table 1, with keeping $[GLC]_{feed}$ = 110.96 mmol L^{-1}. The perturbation is transmitted via the glycolytic, and PPP reaction chain, each species displaying a concentration "peak" not exceeding 4 mmol L^{-1} in the G6P and PYR cases, the system eventually recovers homeostatic steady state. The ChassM prediction error of ca. 25 % (sometimes higher, i.e. 40–100 % for some species[15]) is acceptable being experimentally checked under both stationary and dynamic conditions. The strongest part of the model refers to the valuable link between the PTS glucose import system and the control of the glycolytic pool concentrations of PEP and PYR.

In spite of the previously mentioned limitations, ChassM has proved to be a worthy instrument in developing extended simulation platforms of complex metabolic pathways,[19,46–47] aiming at improving the synthesis rate of a desired metabolite by applying a multi-objective optimization approach.[24,47]

Table 1 – *Parameters of the E. coli cell culture used in simulations (imported values from Chassagnole et al.[16] except for $[GLC]_{feed}$)*

Parameter	Value
Biomass concentration (C_x)	8.7 gDW L^{-1} culture volume
Cell content dilution rate (D)	$1.667 \cdot 10^{-3}$ min^{-1}
Culture dilution rate (F_L/V_L)	$1.667 \cdot 10^{-3}$ min^{-1} (adjusted to be identical to D)
Glucose feeding solution concentration $[GLC]_{feed}$	50 mmol L^{-1} 110.96 mmol L^{-1} (nominal, ChasssM) 21.651, 110.96, 200, mmol L^{-1} (this paper to *in silico* generated data).
Biomass density (ρ_x)	565.5 gDW (L cytosol)$^{-1}$

Termonia and Ross glycolysis model – some tests and a few completions

A valuable reduced model for glycolysis in *E. coli* has been proposed by Termonia and Ross,[30,31] trying to highlight the determinant role played by the ATP/ADP ratio and of the total adenine nucleotide concentration [A(MDT)P] in driving stationary, oscillatory, or unstable evolution of the glycolytic species. The 'core' reaction scheme of Fig. 1 (right) and Table 2 (parameters of the last column), together with the Michaelis-Menten (M-M) or allosteric rate expressions (assuming a cooperative substrate binding over n or m active protomers of the PFK-ASE and PK-ASE) attempt to reproduce not only the activity of the main enzymes (HK-ASE, PFK-ASE, PK-ASE, ATP-ASE) but also the role of PFK-ASE and PK-ASE as oscillation "nodes"[48] by inducing two adverse (negative and positive) backward and forward regulatory loops on the same two interconnected reactions: I) a backward activation with AMP (in equilibrium with ADP) concomitantly with a forward inhibition with ATP of the F6P → FDP and, ii) a backward inhibition with ATP concomitantly with a FDP forward activation of the PEP → PYR reaction. The modelled oscillatory node of PFK reproduces the activation role played by ADP but also by FDP, as proved in the literature.[35]

The TRM model is based on the following simplificatory hypotheses[30,31] (Fig. 1-right):

i) The G6P-to-F6P reaction quickly reaches its equilibrium, being considered together with GLC-to-G6P reaction in the model;

ii) All intermediate steps of FDP-to-PEP pathway (see Fig. 1 – left) have been lumped in only one reversible reaction;

iii) ATP + AMP ⇔ 2 ADP is considered a very fast equilibrium reaction;

iv) The total adenine nucleotide [A(MDT)P] is nearly constant being related to cell resources, and displaying a slow change vs. environmental conditions;

v) The PTS reaction of GLC-to-F6P (V_1 in Fig. 1 and Table 2) is considered constant, the TRM model being thus decoupled from the bioreactor dynamic model. Consequently, concentrations of GLC and products derived from PYR are considered at a constant level.

In spite of such strong hypotheses, most of the TRM parameters fitted by Termonia and Ross[30,31] match the values recommended in literature for various organisms (not necessarily *E. coli* bacteria, but also cells from yeast, brain, muscle, liver, erythrocytes, *S. carlsbergensis*).

The main value of the TRM model derives from its remarkable property to accurately reproduce the oscillatory behaviour of the glycolytic

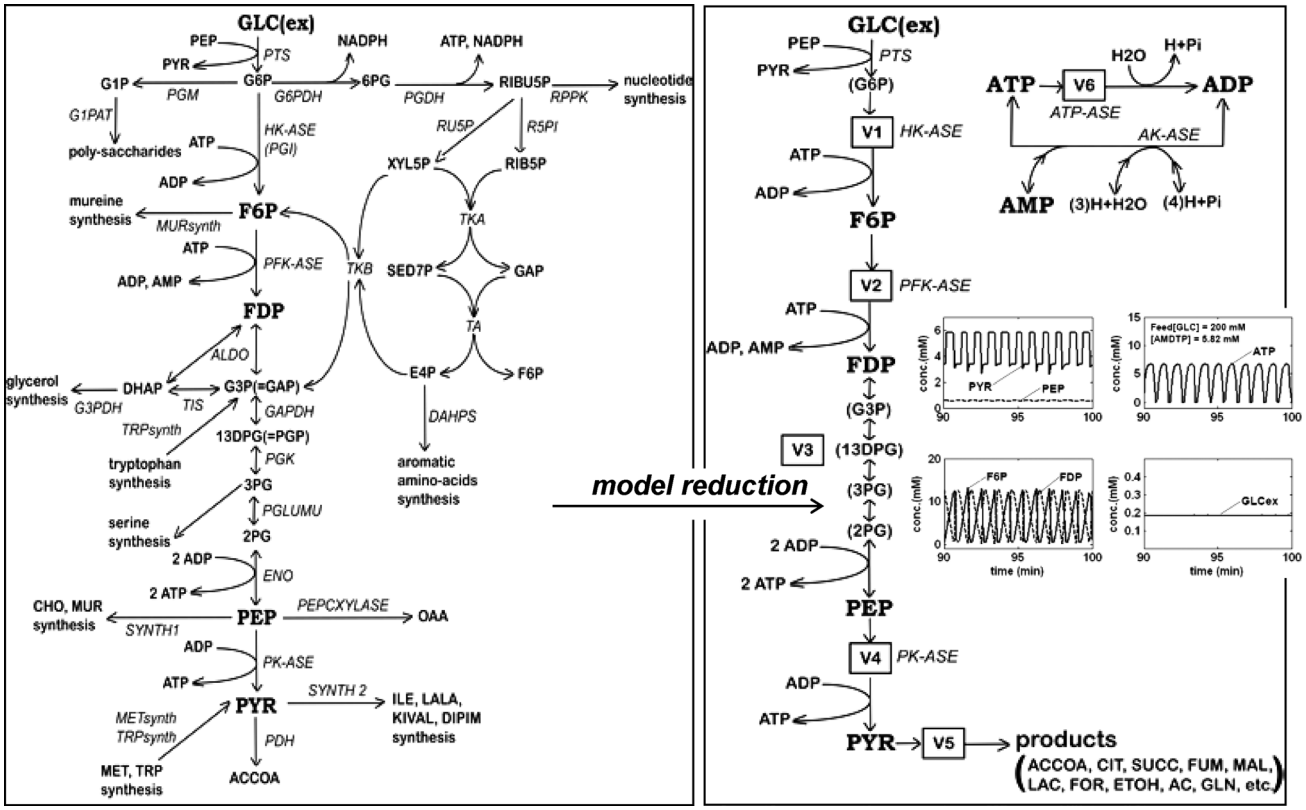

Fig. 1 – *Extended and simplified reaction schemes of glycolysis in E. coli used by: (left scheme) ChassM extended model, including PPP (adapted from Chassagnole et al.[16]); (right scheme) mTRM reduced model, including adenosin co-metabolites ATP, ADP, AMP synthesis. Squares include notations of enzymatic reactions in the mTRM (right). Species in parenthesis are not explicitly included in the mTRM model. Italic letters denote the enzymes.*

pathway under certain environmental conditions (constant V_1 glucose input flux via PTS system), and certain values of the model parameters reflecting the mutual kinetic coupling of the two mentioned nonlinear processes, leading to oscillations propagating over the whole cell metabolism. For instance, by using the original rate constants of Termonia and Ross[30,31] from Table 2 (last column), oscillatory behaviour of a small period (0.2–0.5 minutes) involving the main glycolytic species and fluxes (Fig. 3) occurs when enough A(MDT)P exists and for small ATP/ADP ratios, the adenine nu-

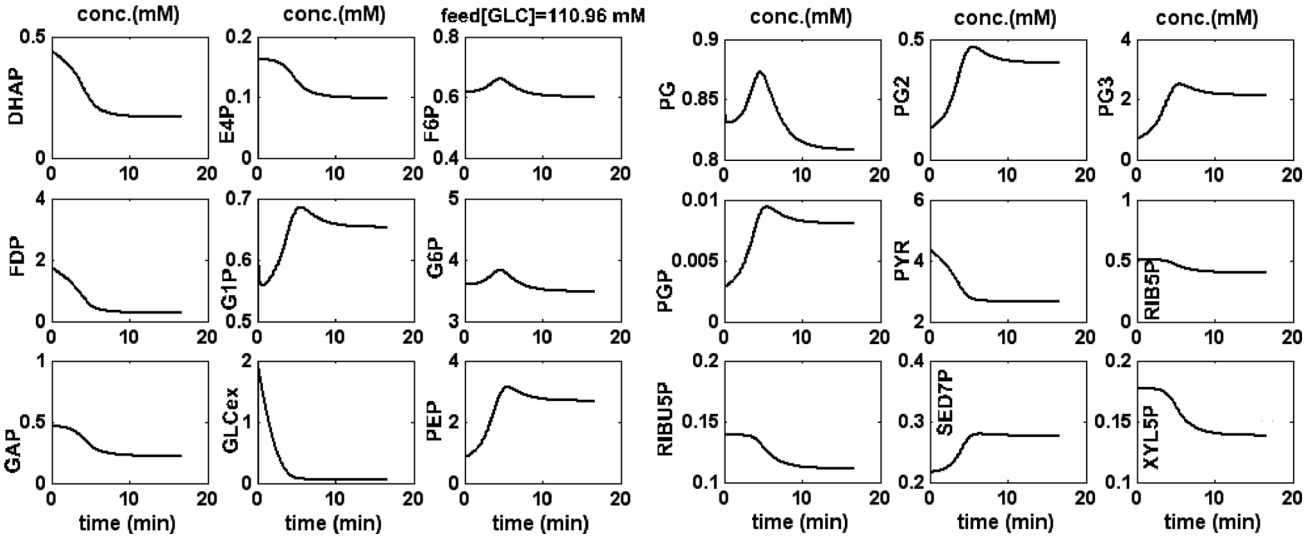

Fig. 2 – *Typical species concentration dynamics in E. coli generated in silico using the ChassM model (——) after an impulse-perturbation in the environmental glucose level ([GLCex] = 2 mmol L^{-1} at time = 0) under nominal bioreactor conditions of Table 1 ($[GLC]_{feed}$ = 111 mmol L^{-1})*

Table 2 – *Original (TRM) and modified glycolysis kinetic model (mTRM) of Termonia and Ross,[30] its re-estimated parameters over a wide range of glucose concentrations in the feeding solution ($[GLC]_{feed}$ = 50–200 mmol L^{-1}), and comparison with literature data*

LITERATURE INFORMATION AND METHODS

– ChassM[16] (Note a) use the same r_{PTS} rate expression with the following parameters:

$$[\, r_{PTS}^{\max}, K_{PTS,a1}, K_{PTS,a2}, K_{PTS,a3}, K_{PTS,G6P}, {}^{n_{PTS,G6P}}] = [7829.78, 3082.3, 0.01, 245.3, 2.15, 3.66], \text{(mmol L}^{-1}\text{, s)}$$

– Ceric & Kurtanjek[36] (Note a) rate expression:

$$r_{PTS} = \frac{r_{PTS}^{\max} c_{GLC}^{ext} c_{PEP}}{(K_{mGLC,\mathrm{PTS}} + c_{GLC})(K_{mPEP,\mathrm{PTS}} + c_{PEP})(K_{iG6P,\mathrm{PTS}} + c_{G6P})^{nPTS}}$$

$$[\, r_{PTS}^{\max}, K_{mGLC,\mathrm{PTS}}, K_{mPEP,\mathrm{PTS}}, K_{iG6P,\mathrm{PTS}}, nPTS] = [1.336, 1.0943, 0.0067, 0.4309, 3.7678], \text{(mmol L}^{-1}\text{, s)}$$

– Usuda et al.[21] (Note a):PTS system of 5 successive reactions of complex Michaelis-Menten kinetics;

– Kadir et al.[28] (Note a) use the same ChassM r_{PTS} expression:

$$[\, r_{PTS}^{\max}, K_{PTS,a1}, K_{PTS,a2}, K_{PTS,a3}, K_{PTS,G6P}, {}^{n_{PTS,G6P}}] = [25.739 \text{ mmol (gDW)}^{-1}\text{ h}^{-1}, 1, 0.01, 1, 0.5, 4], \text{(mmol L}^{-1}\text{)}$$

– Degenring et al.[14] (Note a) rate expression:

$$r_{PTS} = k_{f,PTS}(c_{GLC}^{ext})^{n_{PTS1}} c_{PEP}^{n_{PTS2}} - k_{b,PTS} c_{G6P}^{n_{PTS3}} c_{PYR}^{n_{PTS4}};$$

$$[\, k_{f,PTS}, k_{b,PTS}, n_{PTS1}, n_{PTS2}, n_{PTS3}, n_{PTS4}] = [4.358, 0.814, 0.996, 1.053, 1.183, 0.141], \text{(mmol L}^{-1}\text{, s)}$$

– Westermark & Lansner[35] (Note a):

$$r_{PTS} = \frac{r_{PTS}^{\max} (c_{GLC}^{ext} / S_{0.5}^{GK})^{h_{GK}}}{1 + (c_{GLC}^{ext} / S_{0.5}^{GK})^{h_{GK}}}, \quad [\, r_{PTS}^{\max}, S_{0.5}^{GK}, h_{GK}] = [10 \text{ μmol (gDW)}^{-1}\text{ min}^{-1}, 8 \text{ mmol L}^{-1}, 1.7]$$

RESULTS

Kinetic model parameters

Reaction

$$\text{GLC + PEP} \rightarrow \text{F6P + PYR}$$

$$\text{PYR + ATP} \rightarrow \text{PEP + ADP + H}$$

$$\text{GLC + ATP} \rightarrow \text{F6P + ADP +H}$$

$$V_1 = r_{PTS} = \frac{\rho_x}{C_x} \cdot \frac{r_{PTS}^{\max} c_{GLC}^{ext} c_{PEP} / c_{PYR}}{\left(K_{PTS,a1} + K_{PTS,a2}\frac{c_{PEP}}{c_{PYR}} + K_{PTS,a3} c_{GLC}^{ext} + c_{GLC}^{ext}\frac{c_{PEP}}{c_{PYR}}\right)\left(1 + \frac{c_{G6P}^{n_{PTS,G6P}}}{K_{PTS,G6P}}\right)}$$

Modification: $c_{G6P} = k c_{F6P}$, (Note b)

Proposed mTRM (units in mmol L^{-1}, min)	Original TRM (organism)
$r_{PTS}^{\max}$ = 308.8587	V_1 = 2 mmol L^{-1} min^{-1} (adjustable; no rate constant)
$K_{PTS,a1}$ = 1.0260	
$K_{PTS,a2}$ = 3740.091	
$K_{PTS,a3}$ = 5911.072	
$K_{PTS,G6P}$, $^{n_{PTS,G6P}}$ = absent	
k = 5.8	

LITERATURE INFORMATION AND METHODS

– Chassagnole et al.[16] r_{PFK} rate expression:

$$\frac{r_{PFK}^{\max} c_{ATP} c_{F6P}}{(c_{ATP} + K_{PFK,ATP,s}(1 + \frac{c_{ADP}}{K_{PFK,ADP,c}}))(c_{F6P} + K_{PFK,F6P,s}\frac{A}{B})(1 + \frac{L_{PFK}}{D^{n_{PFK}}})}$$

$$A = 1 + \frac{c_{PEP}}{K_{PFK,PEP}} + \frac{c_{ADP}}{K_{PFK,ADP,b}} + \frac{c_{AMP}}{K_{PFK,AMP,b}};\ B = 1 + \frac{c_{ADP}}{K_{PFK,ADP,a}} + \frac{c_{AMP}}{K_{PFK,AMP,a}};\ D = 1 + \frac{c_{F6P}}{K_{PFK,F6P,s}(A/B)}$$

$$[\, r_{PFK}^{\max}, K_{PFK,F6P,s}, K_{PFK,ATP,s}, K_{PFK,PEP}, K_{PFK,ADP,a}, K_{PFK,ADP,b}, K_{PFK,ADP,c}, K_{PFK,AMP,a}, K_{PFK,AMP,b}, L_{PFK}, n_{PFK} \} =$$

$$= [1840.58, 0.325, 0.123, 3.26, 128, 3.89, 4.14, 19.1, 3.2, 5629067, 11.1],\ (\text{mmol L}^{-1}, \text{s})$$

– Kadir et al.[28] use a similar rate expression:

$$[\, r_{PFK}^{\max}, K_{PFK,F6P,s}, K_{PFK,PEP}, K_{PFK,ADP,AMP,a}, K_{PFK,ADP,AMP,b}, L_{PFK}, n_{PFK}] =$$

$$= [24.613\ \text{mmol (gDW)}^{-1}\ \text{h}^{-1}, 0.14, 3.26, 1.1118, 98.88, 1000, 4],\ (\text{mmol L}^{-1})$$

– Degenring et al.[14] indicate very complex r_{PFK} rate expressions; Usuda et al. (2010) do not supply parameter values.

– Westermark & Lansner[35] (Note a):

$$r_{PFK} = \frac{r_{PFK}^{\max}(c_{F6P}/S_{0.5}^{PFK})^{h_{PFK}}}{(c_{F6P}/S_{0.5}^{PFK})^{h_{PFK}} + \dfrac{1 + ((S_{0.5}^{FBA}/X_{0.5})(c_{FBP}/S_{0.5}^{FBA}))^{h_{FBP}}}{1 + (\beta^{-h_{PFK}^{*}})((S_{0.5}^{FBA}/X_{0.5})(c_{FBP}/S_{0.5}^{FBA}))^{h_{FBP}}}}$$

$[\, r_{PFK}^{\max}, S_{0.5}^{PFK}, S_{0.5}^{FBA}, X_{0.5}, h_{PFK}, h_{FBP}, h_{act}, \beta\,] = [100\ \mu\text{mol (gDW)}^{-1}\ \text{min}^{-1}, 4\ \text{mmol L}^{-1}, 5\ \mu\text{mol L}^{-1}, 10\ \mu\text{mol L}^{-1}, 2.5, 2.5, 1, 5]$,

where:

$$h_{PFK}^{*} = h_{PFK} - (h_{PFK} - h_{act})\frac{(S_{0.5}^{FBA}/X_{0.5})(c_{FBP}/S_{0.5}^{FBA})}{1 + (S_{0.5}^{FBA}/X_{0.5})(c_{FBP}/S_{0.5}^{FBA})}$$

RESULTS

Kinetic model parameters

Reaction

F6P + ATP → FDP + ADP + H

$$V_2 = r_{PFK} = \frac{(V_1/V_{2m})\, c_{F6P}^{\delta}}{\left(K_{2m}^{\delta} + K_{2m}^{\delta}\left[\dfrac{K_R^{AMP}}{K_T^{ATP}}\right]^n \left(\dfrac{c_{ATP}}{c_{AMP}}\right)^n + c_{F6P}^{\delta}\right)}$$

Proposed mTRM (units in mmol L^{-1}, min)	Original TRM (organism)
δ = 1.0437	2 (Note c)
n = 2	2 (muscle)
V_{2m} = 0.062028 (Note d)	V_1 / 0.16 (yeast)
K_{2m} = 6.16423	0.04 (brain)
K_R^{AMP} = 25 μmol L^{-1}	25 μmol L^{-1} (*E. coli*)
K_T^{ATP} = 60 μmol L^{-1}	60 μmol L^{-1} (*E. coli*)

LITERATURE INFORMATION AND METHODS

– Chassagnole et al.[16] (ChassM) use six successive reversible reactions of complex Michaelis-Menten rate expression:

r_{ALDO} and r_{TIS} for (FDP ⇔ GAP/DHAP), r_{GAPDH} for (GAP ⇔ PGP), r_{PGK} for (PGP ⇔ 3PG),

r_{PGluMu} for (3PG ⇔ 2PG), r_{ENO} for (2PG ⇔ PEP).

– Ceric and Kurtanjek[36] use three successive reversible reactions of complex Michaelis-Menten rate expression:

r_{ALDO} and r_{TIS} for (FDP ⇔ GAP/DHAP), and r_{GAPPEP} for (GAP ⇔ PEP).

– Usuda et al.[21] use six successive reversible reactions of complex Michaelis-Menten rate expression:

r_{FBA} and r_{TPI} for (FDP ⇔ GAP/DHAP), r_{GAP} for (GAP ⇔ PGP), r_{PGK} for (PGP ⇔ 3PG),

r_{PGM} for (3PG ⇔ 2PG), r_{ENO} for (2PG ⇔ PEP).

– Kadir et al.[28] use two successive reversible reactions of complex Michaelis-Menten rate expression:

r_{ALDO} for (FDP ⇔ GAP/DHAP), and r_{GAPDH} for (GAP/DHAP ⇔ PEP).

– Degenring et al.[14] use three successive irreversible reactions of complex Michaelis-Menten rate expression:

r_{ALDO} and r_{TIM} for (FDP ⇔ GAP/DHAP), and r_{GAP} for (GAP ⇔ PEP)

(the last resulting from multiplication of the four intermediate step rates):

$$r_{ALDO} = \frac{V_{ALDO}^{\max} c_{FDP}^{n_{ALDO,1}} (c_{G3P} / K_{G3P,ALDO})^{n_{ALDO,2}}}{K_{m,ALDO}^{n_{ALDO,1}} + c_{FDP}^{n_{ALDO,1}}};$$

$$[V_{ALDO}^{\max}, K_{G3P,ALDO}, K_{m,ALDO}, n_{ALDO,1}, n_{ALDO,2}] = [0.897, 0.811, 4.991, 3.091, 2.671], (\text{mmol L}^{-1}, \text{s})$$

$$r_{GAP} = \frac{V_f^{GAP-PEP} c_{GAP} c_{NAD} c_{ADP}}{(K_{m,GAP}^{GAP-PEP} + c_{GAP})(K_{m,NAD}^{GAP-PEP} + c_{NAD})(K_{m,ADP}^{GAP-PEP} + c_{ADP})};$$

$$[V_f^{GAP-PEP}, K_{m,GAP}^{GAP-PEP}, K_{m,NAD}^{GAP-PEP}, K_{m,ADP}^{GAP-PEP}] = [1.929, 3.672, 4.29, 6.783], (\text{mmol L}^{-1}, \text{s})$$

– Westermark and Lansner[35] use two successive reversible reactions r_{FBA} and r_{TPI} for (FDP ⇔ GAP/DHAP), and one irreversible reaction r_{GAP} for (GAP ⇔ PEP) of complex Michaelis-Menten rate expression.

RESULTS

Kinetic model parameters

Reaction

FDP + 2 ADP (+ 2 NAD + 2 P) ⇔ 2 PEP + 2 ATP (+ 2 NADH + 2 H + 2 H2O)

$$V_3 = k_3 c_{FDP}^{\alpha} - k_{3p} c_{PEP}^{\beta}$$

Proposed mTRM (units in mmol L^{-1}, min)	Original TRM (organism)
$k_3 = 73.63477$	5.8; 2.5
$k_{3p} = 337.0371$	0.01
$\alpha = 0.05$	0.05
$\beta = 3$	3 (6)

LITERATURE INFORMATION AND METHODS

– Chassagnole et al.[16] r_{PK} rate expression:

$$\frac{r_{PK}^{\max} c_{PEP} (c_{PEP} / K_{PK,PEP} + 1)^{n_{PK}-1} c_{ADP}}{K_{PK,PEP} \left(L_{PK} \left(\frac{1 + \frac{c_{ATP}}{K_{PK,ATP}}}{1 + \frac{c_{AMP}}{K_{PK,AMP}} + \frac{c_{FDP}}{K_{PK,FDP}}} \right)^{n_{PK}} + \left(1 + \frac{c_{PEP}}{K_{PK,PEP}} \right)^{n_{PK}} \right) (c_{ADP} + K_{PK,ADP})}$$

$[r_{PK}^{\max}, K_{PK,PEP}, K_{PK,ATP}, K_{PK,ADP}, K_{PK,AMP}, K_{PK,FDP}, L_{PK}, n_{PK}]$ = [0.0611315, 0.31, 22.5, 0.26, 0.2, 0.19, 1000, 4], (mmol L^{-1}, s)

– Kadir et al.[28] use a similar rate expression with the same rate constants, excepting $r_{PK}^{\max}$ = 1.0849 mmol $(gDW)^{-1}$ h^{-1}.

– Degenring et al.[14] indicate very complex r_{PFK} rate expressions; Usuda et al.[21] do not supply parameter values.

$$r_{PK} = \frac{V_{f,PK} (c_{PEP} c_{ADP} - c_{PYR} c_{ATP} / K_{eq,PK}) (K_{i,G6P,PK} / c_{G6P})^{n_{PK,1}} (K_{i,C5P,PK} / c_{C5P})^{n_{PK,2}}}{A + B},$$

(C5P = lumped pool of RIB5P, RIBU5P, XYL5P),

$$A = c_{PEP} c_{ADP} (1 + c_{PYR} / K_{i,PYR,PK}) + K_{m,ADP,PK} (c_{PEP} + K_{i,PEP,PK}) + K_{m,PEP,PK} c_{ADP}$$

$$B = \frac{V_{f,PK}}{V_{r,PK} V_{eq}} \left(K_{m,ATP,PK} c_{PYR} (1 + \frac{c_{PEP}}{K_{i,PEP,PK}}) + c_{ATP} \left[K_{m,PYR,PK} \left(1 + \frac{K_{m,PEP,PK} c_{ADP}}{K_{i,PEP,PK} K_{m,ADP,PK}} \right) + c_{PYR} \left(1 + \frac{c_{ADP}}{K_{i,ADP,PK}} \right) \right] \right)$$

$[V_{f,PK}, \ _{eq\ PK}, K_{i,PYR,PK}, K_{m,ADP,PK}, K_{i,pep,pk}, K_{i,PEP,PK}, V_{r,PK}, K_{m,ATP,PK}, K_{m,PYR,PK}, K_{i,ADP,PK}, K_{i,G6P,PK}, K_{i,C5P,PK}, n_{PK,1}, n_{PK,2},]$ =

= [1.113, 0.801, 1.259, 1.01, 0.391, 1.094, 2.444, 0.799, 0.107, 2.232, 1.03, 1.949, 2.074, 0.089], (mmol L^{-1}, s)

RESULTS

Kinetic model parameters

Reaction

$$\text{PEP + ADP + H} \rightarrow \text{PYR + ATP}$$

$$V_4 = r_{PK} = \frac{(V_1 / V_{4m}) c_{PEP}^{\gamma}}{\left(K_{4m}^{\gamma} + K_{4m}^{\gamma} \left[\frac{K_R^{FDP}}{K_{T,PK}^{ATP}} \right]^m \left(\frac{c_{ATP}}{c_{FDP}} \right)^m + c_{PEP}^{\gamma} \right)}$$

Proposed mTRM (units in mmol L^{-1}, min)	Original TRM (organism)
γ = 1.33188	1 (*S. carlsbergensis*)
m = 4	4 (*S. carlsbergensis*)
V_{4m} = 0.13336 (Note d)	V_1 / 0.02 (yeast)
K_{4m} = 1.14644	0.6 (liver)
K_R^{FDP} = 0.2 mmol L^{-1}	0.2 (*S. carlsbergensis*)
$K_{T,PK}^{ATP}$ = 9.3 mmol L^{-1}	9.3 (*S. carlsbergensis*)

LITERATURE INFORMATION AND METHODS

– Chassagnole et al.[16] use two parallel reactions for PYR consumption, r_{Synth2} and r_{PDH}, of Michaelis-Menten rate expression:

$$r_{Synth2} = \frac{r_{Synth2}^{max} c_{PYR}}{K_{Synth2,PYR} + c_{PYR}}; \; r_{PDH} = \frac{r_{PDH}^{max} c_{PYR}^{n_{PDH}}}{K_{PDH,PYR} + c_{PYR}^{n_{PDH}}};$$

$[\, r_{Synth2}^{max}, \; K_{Synth2,PYR} \,] = [0.0736186, 1]$, (mmol L^{-1}, s); $[\, r_{PDH}^{max}, K_{PDH,PYR}, n_{PDH} \,] = [6.05953, 1159, 3.68]$, (mmol L^{-1}, s)

– Kadir et al.[28] use only one reaction for PYR consumption r_{PDH} (PYR → ACCOA), of a complex Michaelis-Menten rate expression; Usuda et al.[21] include three PYR consumption reactions (no parameter supplied).

– Degenring et al.[14] use only one reaction for PYR consumption r_{PDH} (PYR → ACCOA), of a complex Michaelis-Menten rate expression:

$$r_{PDH} = \frac{V_{f,PDH} \; c_{PYR} c_{NAD}}{(K_{m,PYR,PDH} + c_{PYR})(K_{m,NAD,PDH} + c_{NAD})(K_{i,ACCOA,PDH} + c_{ACCOA})^{n_{PDH}}}$$

$[\, V_{f,PDH}, K_{m,PYR,PDH}, K_{m,NAD,PDH}, K_{i,ACCOA,PDH}, n_{PDH} \,] = [0.996, 0.996, 0.996, 0.998, 1.696]$, (mmol L^{-1}, s)

RESULTS

Kinetic model parameters

Reaction

PYR → products (ACCOA, CIT, SUCC, LAC, ETOH, AC, …)

$$V_5 = \frac{k_5 c_{PYR}^{n_{consum,PYR}}}{K_{consum,PYR} + c_{PYR}}$$

Proposed mTRM (units in mmol L^{-1}, min)	Original TRM (organism)
k_5 = 693.3544	1 (adopted)
$K_{consum,PYR}$ = 395.525	–
$n_{consum,PYR}$ = 2.68139	–

LITERATURE INFORMATION AND METHODS

– Chassagnole et al.[16] do not include reactions that interconnect the adenine nucleotide compounds ATP, ADP, AMP (experimental data are used instead).

– The same approach for other glycolytic models, e.g. Ceric & Kurtanjek[36], Usuda et al.[21], Kadir et al.[28], Westermark & Lansner[35]

RESULTS

Kinetic model parameters

Reaction

ATP → ADP +H

$$V_6 = k_6 c_{ATP}$$

Proposed mTRM (units in mmol L^{-1}, min)	Original TRM (organism)
k_6 = 4025.351	0.1 (rat erythrocytes)

LITERATURE INFORMATION AND METHODS

Termonia and Ross[30] indicate experimental evidence of a very fast reversible reaction catalysed by *AKASE*, the equilibrium being quickly reached.

RESULTS

Kinetic model parameters

Reaction

$$2\ \mathrm{ADP} \leftrightarrow \mathrm{ATP} + \mathrm{AMP}$$

$$c_{ATP}c_{AMP} = Kc_{ADP}^2$$

Proposed mTRM (units in mmol L^{-1}, min)	Original TRM (organism)
$K = 1$	1

Footnotes:

(a) Separate rate expressions for the two reactions (r_{PTS} and r_{PGI})(see Fig. 1 – left).

(b) The $c_{G6P} = kc_{F6P}$ proportionality tries to overcome the lack of the r_{PGI} rate expression in the mTRM.

(c) Constants δ and n present the same value in the original TRM.[30] In the mTRM, they display different values by similarity with the V_4 expression.

(d) The stationary V_1 flux in Chassagnole et al.[16] simulated experiments is larger than that of the Termonia and Ross,[30] which is 5.4157 mmol L^{-1} min^{-1} (cyt) for $[GLC]_{feed}$ = 50 mmol L^{-1} (environment), 12.017 mmol L^{-1} min^{-1} (cyt) for $[GLC]_{feed}$ = 110.96 mmol L^{-1} (environment), and 21.651 mmol L^{-1} min^{-1} (cyt) for $[GLC]_{feed}$ = 200 mmol L^{-1} (environment).

cleotide playing one of the essential roles in generating self-sustainable oscillations.

Heyland et al.[49] experimentally proved the limited resources of adenine nucleotides in a cell, even if internal control circuits are constantly changing ATP/ADP/AMP ratios, trying to compensate the metabolic burden by enhancing the production of ACCOA and acetate allowing NADH and ATP synthesis via TCA cycle, concomitantly with the conversion of NADPH excess in NADH (through oxidative phosphorylation, not included in the TRM). Such a complex inter-dependence between energy resources and free-energy dissipation was considered by Termonia and Ross[30,31] in a simple way, by including only two reactions (Table 2, last rows) by which ATP is converted to ADP, while ADP quickly reaches its equilibrium state vs. ATP and AMP, the sum of adenine nucleotide concentrations [A(MDT)P] remaining all times constant (see the mass balances of Table 3). Experimental proof of such qua-

Table 3 – *Bioreactor and glycolysis mass balance equations for the mTRM model*

Species mass balance	Auxiliary relationships
$\frac{dc_{GLC}^{ext}}{dt} = D\left(c_{GLC}^{feed} - c_{GLC}^{ext}\right) - \frac{C_x}{\rho_x}V_1$	
$\frac{dc_{F6P}}{dt} = V_1 - V_2 - D\ c_{F6P}$	
$\frac{dc_{FDP}}{dt} = V_2 - V_3 - D\ c_{FDP}$	i) $c_{AMP} + c_{ADP} + c_{ATP} = c_{AMDTP}$ = constant;[30]
$\frac{dc_{PEP}}{dt} = 2\ V_3 - V_4 - D\ c_{PEP}$	ii) c_{ADP} results from solving the thermodynamic equilibrium relationship $c_{ATP}c_{AMP} = Kc_{ADP}^2$, that is: $c_{ADP}^2\frac{K}{c_{ATP}} + c_{ADP} - c_{AMDTP} + c_{ATP} = 0$
$\frac{dc_{PYR}}{dt} = V_4 - V_5 - D\ c_{PYR}$	iii) $y_{SUCC} \approx 1/38$ (from the GLC/ATP stoichiometric coefficient[54])
$\frac{dc_{ATP}}{dt} = -V_1 - V_2 + 2\ V_3 + V_4 - V_6 - D\ c_{ATP}$	
$\frac{dc_{SUCC}}{dt} \approx y_{SUCC}\frac{dc_{ATP}}{dt}$	

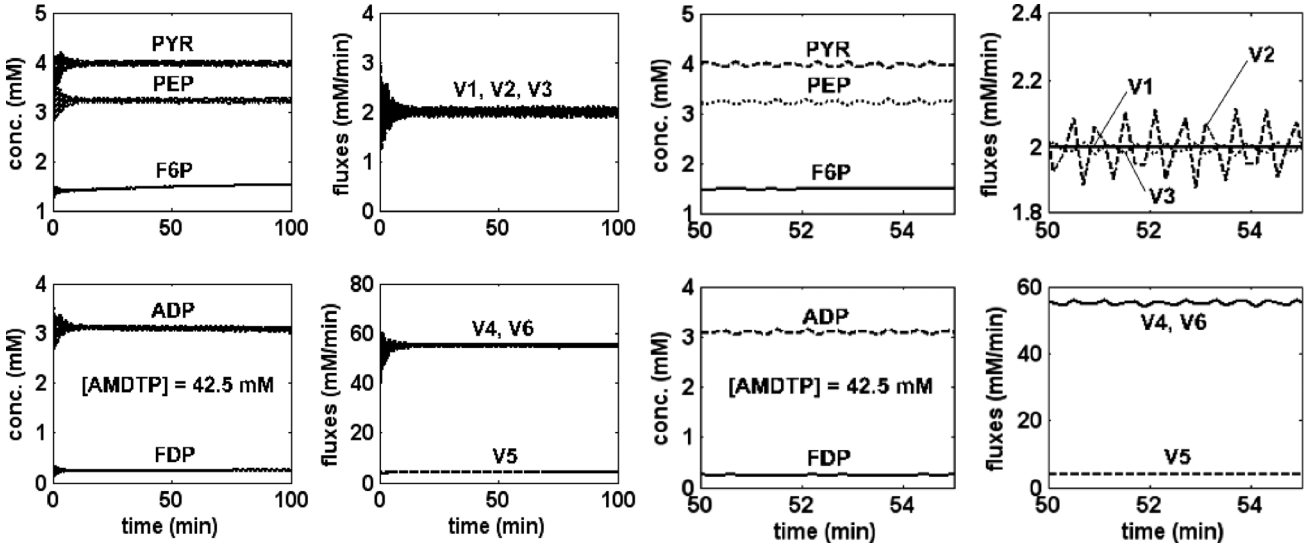

Fig. 3 – *Predictions of the original TRM model (Table 2, last column) concerning species concentrations and metabolic fluxes under stationary oscillations in E. coli, over a longer (left) or shorter (right) time-window for [AMDTP] = 42.5 mmol L^{-1}, V_1 = 2 mmol L^{-1} min^{-1}, and D = 1.667·10^{-3} min^{-1}*

si-constancy of [A(MDT)P] in *E. coli* is offered by Chassagnole et al.[16] dynamic data obtained after a pulse perturbation in the GLC substrate.

A few modifications of the TRM have been proposed in the present study, leading to the mTRM, in order to improve its adequacy vs. ChassM over a large bioreactor operating domain, as follows:

i) The constant inlet glucose flux V_1 in Table 3 mass balance was replaced by the ChassM extended M-M expression of Table 2 for glucose symport PTS to account for the PEP/PYR ratio and external GLC level of influence on the PTS.[34]

ii) As G6P is not explicitly included in the model, it was replaced by the $c_{g6p} = kc_{f6p}$ proportionality, with constant k to be identified. Preliminary observations pointed out the quasi-constancy of [G6P]/[F6P] ratio over a wide range of external [GLCex) levels.

iii) In contrast to the original TRM, the constant δ in the V_2 rate expression was considered at taking different values from n, similarly to different values of γ and m constants in V_4 rate expression of TRM. The assumption is that the number (n or m) of ligand molecules binding to one molecule of enzyme (PFK-ASE or PK-ASE) depends on the type of ligand, leading to $\left[K_R^{amp} / K_T^{atp}\right]^n$ or $\left[K_R^{fdp} / K_{T,PK}^{atp}\right]^m$ terms in the allosteric control expression of V_2 and V_4 respectively (where K_R and K_T are the dissociation constants for ligands bound to the R and T conformations of PFK-ASE and PK-ASE, respectively). However, due to the applied lumping procedure, the allosteric exponents (δ and γ) of substrate F6P or PEP might have different values than those of the Michaelis-Menten substrate constants K_{2m} and K_{4m}.

iv) The first-order rate V_5 of the PYR consumption in the original TRM was replaced by the M-M expression of ChassM model to roughly account for the consumption rate inhibition with the PYR substrate.

v) To simply illustrate how a metabolic end product synthesis can be attached to the glycolysis pathway, the succinate production is included in the mTRM of Table 3, in a very approximate form, by considering its synthesis concomitantly with the ATP in the TCA cycle, of an average stoichiometry of 1:38 SUCC-to-ATP ratio. A more sophisticated synthesis pathway module of TCA might be used instead, but it is beyond the aim of this study.

The mass balance equations of mTRM are presented in Table 3, and the rate expressions in Table 2.

Parameter adjustment of the proposed mTRM model to fit the ChassM predictions

To ensure a satisfactory adequacy of the proposed mTRM reduced model over a wide bioreactor operation domain, and due to lack of experimental data, the rate constants have been refitted to match the ChassM *m*-key species predictions generated by repeated system simulations under various feeding conditions. Three such bioreactor / cell culture dynamic regimes (N = 3) have been simulated with ChassM, that is $[GLC]_{feed}$ = 110.96 mmol L^{-1}, $[GLC]_{feed}$ = 50, and $[GLC]_{feed}$ = 200 mmol L^{-1}, respectively, by keeping the nominal conditions as in Table 1. The dynamic data sets have been generated by applying each time an initial pulse pertubation of GLC level in the bioreactor from $[GLC]_{ext}$ = 0.055 mmol L^{-1} to $[GLC]_{ext}$ = 2 mmol L^{-1}, similarly to the

experimental perturbation applied to the bioreactor operation employed by Chassagnole et al.[16] during their estimation step.

The mTRM model parameters (vector $\boldsymbol{k}$) have been estimated by minimizing the differences between the mTRM and ChassM predictions in terms of species stationary concentrations, but also in trajectory amplitudes during recovery of steady state after an impulse perturbation of the glucose level in the bioreactor. The two fitting criteria are joined in a multi-objective estimation rule by applying the *weighting function method* with scaled objectives.[50] The solution results from minimization of a composite objective function F that includes the residues between mTRM and ChassM model predictions over the three generated data sets, in terms of relative standard deviations of species stationary concentrations, and of the average relative deviation in species recovering amplitudes,[13] that is in scaled form:

$$\hat{\boldsymbol{k}} = \arg\,\mathrm{Min}\,\Phi = (s_y + w \times s_{ampl}),$$

$$s_y = \sqrt{\sum_{u=1}^{N}\sum_{j=1}^{m}\left(\left(c_{uj,\infty}^{mTRM} - c_{uj,\infty}^{ChassM}\right)/c_{uj,\infty}^{ChassM}\right)^2/(Nm)},$$

j = GLCex, F6P, FDP, PEP, PYR

$$s_{ampl} = \sum_{u=1}^{N}\sum_{j=1}^{m}\left(\left|\mathrm{Max}(c_{uj}^{mTRM}(t)) - \mathrm{Max}(c_{uj}^{ChassM}(t)\right|/\right.$$
$$\left./\mathrm{Max}(c_{uj}^{ChassM}(t))\right)/(Nm),$$

$$\text{s.t. } \hat{\boldsymbol{k}} > 0;\ [\mathrm{AMDTP}]_{\mathrm{mTRM}} = [\mathrm{AMDTP}]_{\mathrm{ChassM}} = \text{constant (imposed)}, \quad (1)$$

where: AMDTP = adenosin-(mono)(tri)phosphate; N = number of ChassM generating "experimental" data sets ($N = 3$); m = number of "observed" mTRM variables ($m = 5$ here); '^' = estimated values, '∞' = stationary value; w = weights in the joint objective function. The adopted weight $w = 0.01$ tries to realize the match of the two models (extended ChassM and reduced mTRM) rather in terms of stationary concentrations of key-species than those in the recovering trajectories of species steady states. The weighting factors in objective function (1) chosen to reflect that glycolysis species stationary levels are very important for the other metabolic syntheses deriving from them.

The adaptive random optimization algorithm MMA of Maria[51] implemented in MATLAB™, was used as an effective solver. The multimodal search was started from the original TRM parameters and those indicated by ChassM, by searching over reasonable parametric ranges of 1–2 orders of magnitude higher/lower than the initial guess (except for k_{3p} which varied over a larger domain).

Estimation was applied to only 17 parameters of mTRM (from the total of 26), that is vector $\boldsymbol{k} = [r_{PTS}^{\max}, K_{PTS,a1}, K_{PTS,a2}, K_{PTS,a3}, k, \delta, V_{2m}, K_{2m}, k_3, k_{3p}, \gamma, V_{4m}, \quad , k_5, K_{consum,pyr}, n_{consum,pyr}, k_6]$, the others being adopted from the values recommended by Termonia and Ross[30,31] as discussed below. The estimate is presented in Table 2. Comparative mTRM vs. ChassM predictions of the stationary conditions at large experimental recovery times after the GLC-pulse-perturbation (i.e. more than 20 minutes) are presented in Fig. 4. It should be mentioned that, for these simulated bioreactor conditions and cell culture characteristics, there is no oscillatory glycolytic process.

By analysing the estimated rate constants of the mTRM comparatively to the literature results (Table 2), several aspects can be underlined.

Reaction V_1. In the PTS rate expression, the G6P inhibition term from denominator can be neglected and $K_{PTS,g6p}$ parameter can be missed. A comparison between mTRM, ChassM and Kadir et al.[28] constants in the V_1 denominator (GLC import noncompetitive inhibition by PEP, PYR, and external GLC) reveals very different values due to the influence of the whole model structure. Comparison with other PTS rate expressions from literature (Table 2) is not easy even if they include similar types of inhibition (with less or more terms). A exception is the power-law rate expression of Degenring et al.[14] which advanced a reversible PTS reaction due to the strong inhibition with PYR and G6P. The adopted constant V_1 for GLC import flux in the basic TRM model appears to be a too strong approximation by missing the various inhibitory effects on PTS, as proved by the very different predicted V_1 values in the three sets of simulated experiments with ChassM (see footnote d of Table 2).

Reactions V_2 *and* V_4. The F6P-to-FDP and PEP-to-PYR reactions can be analyzed together by presenting the same allosteric form of the rate expression, both reactions playing a central role in generating glycolytic oscillations due to the coupled positive and negative regulatory feedback loops acting on the activity of the two enzymes PFK-ASE and PK-ASE (i.e. oscillatory 'nodes'). The number (n or m) of ligand molecules bound to the enzymes (PFK-ASE or PK-ASE), and the K_R and K_T dissociation constants in the control of V_2 and V_4 have been adopted at the TRM values (see discussion of Termonia and Ross;[30,31] also $m = n_{PK} = 4$ of ChassM). The estimated exponent $\delta = 1.04$ in V_2 is half that of TRM but similar to that of ChassM, while $\gamma = 1.33$ in V_4 is very close to that of TRM. The other rate constants (V_{2m}, K_{2m}, V_{4m}, K_{4m}) present estimated

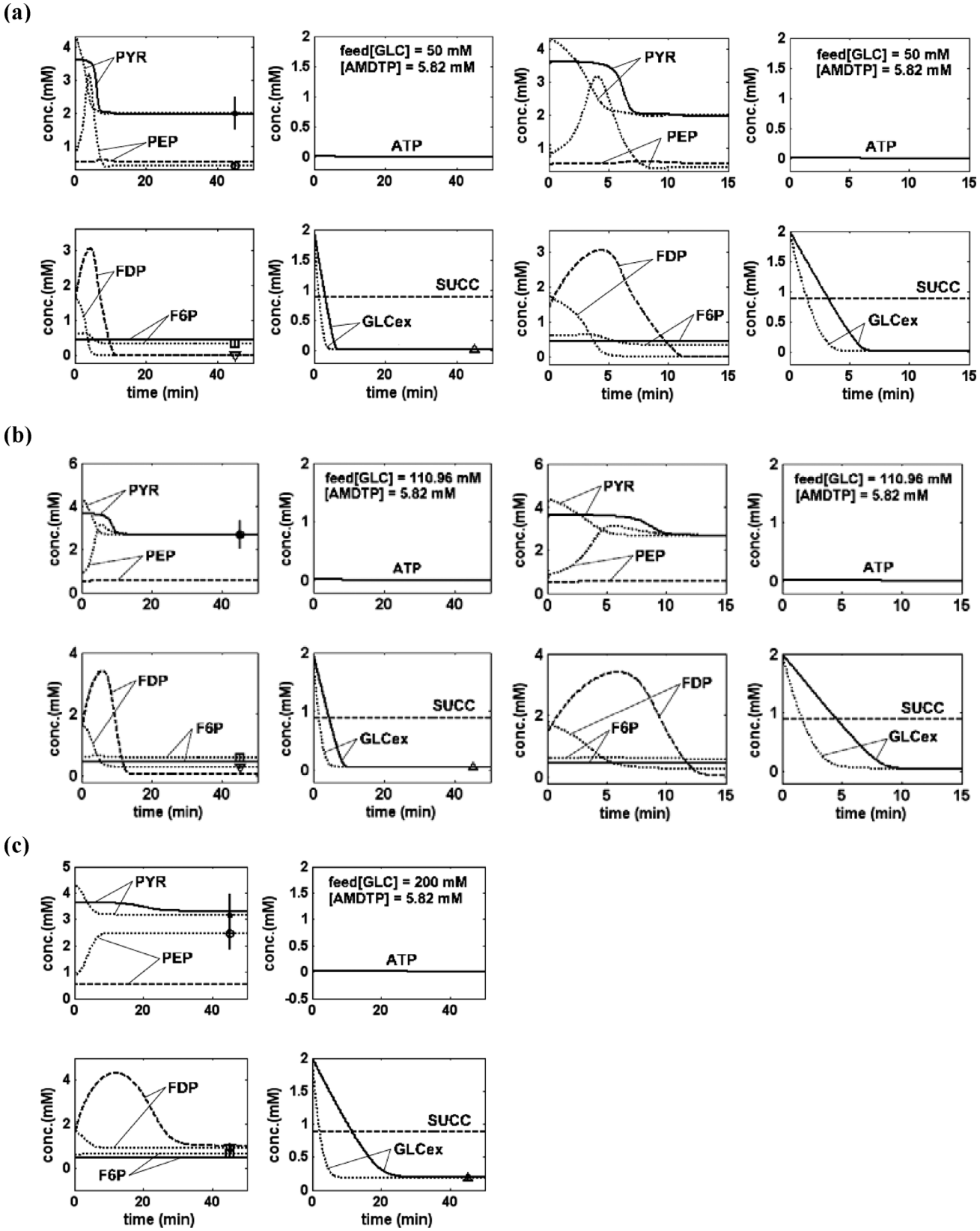

Fig. 4 – *Species concentration dynamics predicted by the modified mTRM model (—— ,----) in E. coli after a pulse-perturbation in the environmental glucose level ([GLCex] = 2 mmol L^{-1} at time = 0). The in silico generated dynamic trajectories (·····) and stationary concentrations (*, ○, □, ▽ symbols) are generated in silico by using the Chassagnole et al.[16] model (ChassM) under the nominal bioreactor operation of Table 1 ([AMDTP] = 5.82 mmol L^{-1}, D = 1.667·10^{-3} min^{-1}), for three different feeding conditions: $[GLC]_{feed}$ = 50 mmol L^{-1} (a), $[GLC]_{feed}$ = 110.96 mmol L^{-1} (b), $[GLC]_{feed}$ = 200 mmol L^{-1} (c). The first two columns from the left include plots in a longer time-window (50 min), while the two right columns include plots in a shorter time-window (15 min).*

values comparable to those of TRM. A comparison of these estimated constants with those of other models listed in Table 2 is difficult due to differences in the rate expressions, even though they present the same order of magnitude.

Reaction V_3. The FDP-to-PEP transformation is considered as a reversible reaction by most of the reported models (Table 2), taken as a lump in TRM or mTRM, or as a succession of 2-to-6 reversible steps. The considered power-law kinetics in mTRM preserves the same values for the reaction orders as in the original TRM, while the estimated (k_3, k_{3p}) constants present larger values due to the much higher GLC input fluxes into the cell in the simulated Chassagnole et al.[16] experiments than those considered by TRM.

Reaction V_5. The PYR consumption in the cell follows a significant number of pathways (e.g. see the classical Edwards & Palsson model discussed by Maria et al.[25]). Such a PYR consumption term is considered in lumped form in the basic TRM and mTRM, while ChassM considers only two parallel consumption reactions (r_{Synth2} and r_{PDH} in Table 2). However, to account for PYR inhibition control, the rate expression in the mTRM was adopted from an M-M type similar to ChassM, the estimated rate constants indicating a high-order ($n_{consum,PYR}$ = 2.68) PYR consumption comparable to those leading to ACCOA synthesis (n_{PDH} = 3.68 in Table 2). Other literature expressions of complex M-M type assume a non-competitive inhibition with PYR and NAD^+ substrates, and ACCOA product.

Reaction V_6 and nucleotides interconversion. Most of the kinetic models from literature (such as ChassM and others, see Table 2) do not explicitly account for the interconversion and equilibrium reactions involving ATP, ADP, and AMP, but instead consider experimental data or constant levels. However, the nucleotide species are the driving force of the glycolytic pathway, and a measure of the total cellular energy dynamics, which plays an essential role in the glycolysis regulation and oscillation occurrence as extensively studied by Termonia and Ross[30,31]. This is why the same ATP/ADP/ATP reaction system was adopted in the mTRM, the estimated k_6 constant being much higher than that of TRM due to the high glycolytic fluxes in the ChassM simulated experiments. However, the equilibrium constant of ADP to ATP and AMP interconversion was kept at the same value (K = 1).

As revealed by the comparative plots of species dynamic trajectories for all three simulated experiments (Fig. 4), the species steady-state concentrations predicted by mTRM and ChassM fairly match. A detailed comparison of bias between the two model predictions given in Table 4 reveals an average relative error of 38 %, which means a plus of ca. 8–13 % to the 25–30 % deviation of ChassM vs. experimental data (reported only for one data set by Chassagnole et al.[16] Such a satisfactory result is quite remarkable if considered together with the large reduction in model parameterization from 127 difficult to identify parameters of ChassM to only 17 easily identifiable parameters of the reduced mTRM (i.e. ca. 7–8-fold reduction in parameter vector size). At the same time, the mTRM fit realized over a wide experimental domain of $[GLC]_{feed}$ = 50 – 200 mmol L^{-1} increases the model value. The bias between the two models is however non-uniformly distributed among species: GLCex and PYR report negligible deviations (below 5 %), F6P and FDP deviations are in the range of ChassM model error of 25–30 %, while only PEP species concentrations reports a larger relative difference of ca. 60 % between the two models. Such a result can be explained by the central role played by PEP in controlling the glycolytic fluxes, its concentration level trying to compensate the effect of lumping of species and reactions in the reduced model. Surprisingly, the mTRM reports lower maximum deviations (of ca. 60 %) comparatively to ChassM maximum deviations vs. experimental data for some species (of ca. 100 %). This relatively low adequacy of the reduced model might be caused by the smaller number of parameters used to reproduce the process high complexity using the same experimental data. This model adequacy can be improved using different rate expressions and adding new model terms.[56]

Dynamic simulations with the identified mTRM given in Fig. 4 reveal moderate species transient amplitudes (smaller than 4 mmol L^{-1}) after an initial impulse in the external glucose, valid for all three simulated feeding conditions. Such results fairly match with ChassM simulations (Fig. 4, dashed lines in the right column of plots), even though the recovering trajectories for some species are different in shape (PEP, FDP) due to the inherent effect of reaction lumping. Also, the steady-state recovering time of ca. 10 minutes is practically the same for both mTRM and ChassM models. The bias in species recovering amplitudes is small (below 20 %) for all species except FDP (68 %).

Finally, the mTRM gain in simplicity and versatility is obtained at the expense of a loss of information about some glycolytic species, and of obtaining max. 60–70 % biased predictions for one or two species under stationary or dynamic operating conditions. However, the obtained mTRM adequacy is very satisfactory (below ChassM extended model error) for all other species, the mTRM model passing the adequacy χ^2-test (i.e. a model variance ratio smaller than the minimum of 3.8 for a 95 % confidence level[13]).

Table 4 – *Differences between mTRM vs. ChassM model predictions, compared to ChassM model relative error vs. experimental data.[16] Notation: QSS = quasi-steady-state*

Species	Relative deviation (%) for QSS concentrations, $\frac{\left\|c_j^{mTRM} - c_j^{ChassM}\right\|}{c_j^{ChassM}}$	Relative deviation (%) for QSS recovering amplitudes, $\frac{\left\|\mathrm{Max}(c_j^{mTRM}) - Max(c_j^{ChassM})\right\|}{\mathrm{Max}(c_j^{ChassM})}$
GLCex	4.2	–
PYR	2.1	16.6
PEP	61.8	10.2
F6P	28.3	19.5
FDP	30.4	68.6
mTRM model relative error standard deviation [(a)]	38.2 % (max. 62 %)	54.0
ChassM model average relative error (vs. experimental data of Chassagnole et al.[16])	ca. 25 % (max. 100 %)	ca. 25 % (max. 100 %)

[(a)] in relative terms, over all data sets and species.

Reduced mTRM model relevance and glycolytic oscillation occurrence

The results obtained with the proposed reduced mTRM must be analysed in more detail to understand the model advantages and limitations, as long as such a reduced, easily identifiable structure might be part of extended metabolic models.

i) Certainly, the considerably reduced identification effort of mTRM model parameters is one of its strongest characteristics as long as extended simulation platforms already include large parameterization. With the expense of a plus of 8–13 % in model deviations vs. ChassM, and a larger deviation in the recovering amplitudes and steady-state levels for 1–2 species, the considerable reduction in the parameter number to only 17, together with a validity over a wide bioreactor operating domain, recommend the mTRM for quick analyses of the central carbon metabolism main fluxes.

ii) Being of simple structure, the mTRM is easily adaptable (less computation intensive) to correlate various data sets from different cell cultures, easily extensible and connectable to other metabolic pathways. Such reduced representations do not replace the large capabilities of the extended metabolic models, but only replace them in quick analyses of parts of cell metabolism, such as substrate utilization, oscillation occurrence, or structured interpretation of metabolic changes in modified cells. Being part of modular constructions, reduced glycolytic models deserve various objectives, e.g. analysis of genetic regulatory circuits controlling synthesis of target metabolites, flux distribution and *in silico* reprogramming of some metabolic pathways, whole cell model studies (e.g. amino acid, succinic acid synthesis), etc.[7,8,10,25,43,46]

iii) The mTRM simplicity is also an advantage for easier characterization of the cell system (stability, responsivity to stimuli, species connectivity, regulatory efficiency) in terms of Metabolic Control Analysis (MCA) definitions (see the MCA indices on the JWS platform of Olivier & Snoep[37], Laiterä[38], Heinrich & Schuster[52] not detailed here).[57,58,43,25,46]

iv) Being less parameterized, the required structured and unstructured information from experiments and –omics data banks by the mTRM identification step is considerably smaller than that necessary for extended models. However, such an advantage is accompanied by inherent model drawbacks, such as: loss in predictive power on certain species and reaction steps; loss in system flexibility given by a reduced number of intermediates and species interactions; lack of physical meaning for some parameters; possible alteration of some systemic properties in terms of recovering trajectory and amplitudes, stability strength, system sensitivity, and regulatory characteristics. As proved by our tests, the bias introduced over the dynamic and stationary simulations of the checked bioreactor case are acceptable.

v) To test the capability of mTRM model to reproduce regulatory characteristics and self-sustainable stationary oscillations in the glycolytic pathway, a modified cell system was analysed. As extensively discussed in the literature, stationary oscillations occurrence depends on the characteristics of the concomitant positive and negative regulatory loops applied to the oscillation 'node' (e.g. enzyme activity characteristics reflected by some rate constant values), being also influenced by the system fluxes (i.e. bioreactor operating conditions).[48] As PFK-ASE and PK-ASE act as oscillation "nodes" for the interconnected reactions

$$F6P \xrightarrow{+ATP} FDP \underset{k_{3p}\ (+ATP+NADH+H+H_2O)}{\overset{k_3\ (+ADP+NAD+P)}{\rightleftharpoons}}$$

$$PEP \xrightarrow{+ADP} PYR,$$

the external conditions inducing certain F6P synthesis flux as well as the ATP/ADP/AMP ratio and total [A(MDT)P] play an essential role in determining the oscillation occurrence in the species concentrations. This is why Termonia and Ross[30,31] varied [A(MDT)P] and k_3 constant to induce cellular oscillations with the basic TRM. For the proposed mTRM model, this 'oscillation engine' can be easily started-up for instance by operating at high cell fluxes (i.e. high input substrate levels in the bioreactor, $[GLC]_{feed}$ = 200 mmol L^{-1}) and for a slower regeneration of ADP (i.e. k_6 = 10 min^{-1} instead of identified 4025.351 min^{-1} from ChassM simulated experiments). The resulting oscillations are plotted in Fig. 5, being of ca. 1 minute period comparable with those of Schaefer et al.[45] Oscillation occurrence here is related to the continuous system perturbation induced by the high GLC external level and assimilation flux requiring PFK-ASE activation, but also to the large amount of ADP for PEP and PYR production. Consequently, the slow ADP recovery from ATP cannot be realized at the same consumption rate, thus resulting in a continuous oscillatory trajectory for ADP, on the same shape with those of ATP. In fact, the oscillatory properties can be modulated by changing the process conditions and some structural characteristics of the cell culture (reflected by the rate constants; see Heinrich & Schuster[52] for an extensive discussion on the mathematical conditions for oscillation occurrence).

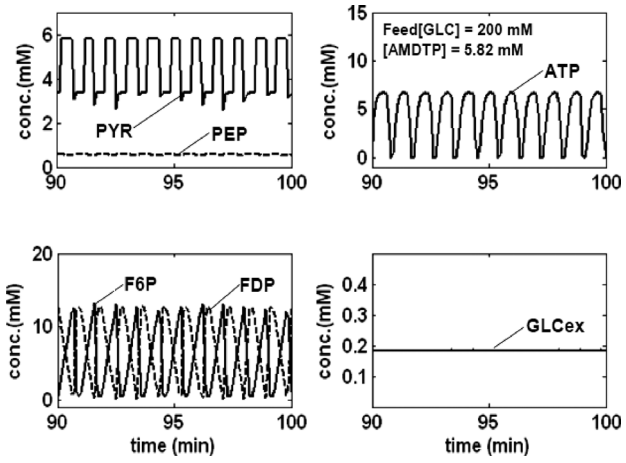

Fig. 5 – *Modified mTRM model (Table 2) predictions of glycolytic stationary oscillations occurrence in E. coli for the bioreactor operating conditions of Table 1 ([AMDTP] = 5.82 mmol L^{-1}, D = 1.667·10^{-3} min^{-1}), for high level feeding conditions of $[GLC]_{feed}$ = 200 mmol L^{-1} and slower ATP → ADP +H reaction rate of k_6 = 10 min^{-1}*

Conclusions

The use of reduced vs. extended kinetic models when modelling complex metabolic pathways is a continuously challenging subject when developing structured cell simulators for various applications (flux analysis, target metabolite synthesis optimization, *in silico* reprogramming of the cell metabolism and design of new micro-organisms, bioreactor / bioprocess optimization). As exemplified by the *E. coli* glycolysis case study, the reduced mTRM model, of simple and easily adaptable structure to various cell cultures, can be used in quick analyses of cell metabolism, such as substrate utilization, oscillation occurrence, or structured interpretation of metabolic changes in modified cells.

Reduced structured models, of satisfactory adequacy (even if rough for 1–2 species) is preferable to other semi-empirical or lumped representations, being easily included in modular cell simulation platforms to be used for solving various objectives, such as analysis of cell adaptation to certain environmental conditions, simulation of genetic regulatory circuits controlling the synthesis of some target metabolites, simulation of flux distribution and its dynamics under transient regimes, *in silico* reprogramming of some metabolic pathways, etc.

At the expense of ca. 8–13 % increase in the relative model error vs. extended simulation models, derivation of reduced kinetic structures to describe some parts of the core metabolism is worth the associated identification effort, due to the considerable reduction in model parameterization (e.g. 17 parameters in mTRM vs. 127 in ChassM), while preserving fair adequacy over a wide experimental domain. When cell characteristics are constantly changing, the reduced model can be quickly upgraded by using experimental information, or predictions of the extended kinetic models such as ChassM. In such a manner, a multi-layer model can be obtained: in a first step an extended model is developed based on extensive experimental data; subsequently, for quick cell process analyses, and optimization purposes, a reduced model can be used instead, and fitted by using the extended model simulations for some 'local' conditions; finally, the cell process complexity appears to be described by a succession of local reduced models "enfolded" in the real process.[43,53]

Being quite versatile, the reduced mTRM model includes enough information to reproduce not only the cell energetic potential through the total A(MDT)P level, but also the role played by ATP/ADP ratio as a glycolysis driving force. The model can also reproduce the oscillatory behaviour occurrence conditions, as well as situations when homeostatic conditions are not fulfilled.

The glycolysis core model can be easily extended by including any complex synthesis and regulatory pathway deriving from the main carbon uptake stream (e.g. the SUCC production here), without necessarily complicating the 'core' model with too many species and parameters of less importance for the target metabolite production.

Generally, the reduced model quality is strongly dependent on the lumping degree, the key-species selection and ability to achieve the suitable trade-off between model simplicity, its predictive power and physical meaning of terms.

ACKNOWLEDGEMENT

I want to thank my wife for helping me publish this paper in a critical situation, being half paralyzed after a severe vascular cerebral attack.

Nomenclature

c_j – species j concentration
C_x – biomass concentration
D – cell content dilution rate (identical to the adjustable culture dilution rate, F_L / V_L)
F_L – liquid feed flow rate in the bioreactor
k_j, K_j, V_{2m}, V_{4m}, $r_j^{\max}$ – rate and equilibrium constants
m – number of observed variables, or rate constant
n – reaction order
N – number of experimental data sets
r_j – species j reaction rate
s_y – standard deviation (in relative terms)
t – time
V_j – metabolic fluxes
V_L – liquid volume in the bioreactor
y_{succ} – stoichiometric coefficient
w – weights in the joint objective function

Greeks

$\alpha, \beta, \gamma, \delta$ – reaction orders
χ – χ – statistical distribution
Φ – composite objective function
ρ_x – biomass density

Superscripts

^ – estimated value

Subscripts

∞ – stationary value

Abbreviations

13DPG, PGP – 1,3-diphosphoglycerate
2PG – 2-phosphoglycerate
3PG – 3-phosphoglycerate
6PG – 6-phosphogluconate
AA – amino-acids
AC – acetate
ACCOA – acetyl-coenzyme A
ACT – Hill coefficient in the limiting case of excess FBP
ADP – adenosin-diphosphate
AK-ASE – adenylate kinase
ALDO – aldolase
AMDTP – adenosin-(mono)(tri)phosphate
AMP – adenosin-monophosphate
ATP – adenosin-triphosphate
ATP-ASE – ATP monophosphatase
ChassM – Chassagnole et al. (2002) model
CHO – chorismate
CIT – citrate
DAHPS – DAHP synthases
DHAP – dihydroxyacetonephosphate
DIPIM – diaminopimelate
DW – dry mass
E4P – erythrose-4-phosphate
ENO – enolase
ETOH – ethanol
F6P – fructose-6-phosphate
FDP – fructose-1,6-biphosphate
FOR – formate
FUM – fumarate
GAPDH – glyceraldehyde-3-phosphate dehydrogenase
G1P – glucose-1-phosphate
G1PAT – glucose-1-phosphate adenyltransferase
G3P, GAP – glyceraldehyde-3-phosphate
G3PDH – glycerol-3-phosphate dehydrogenase
G6P – glucose-6-phosphate
GLC – glucose
G6PDH – glucose-6-phosphate-dehydrogenase
GLCex, GLC[ext] – Glucose in the external environment
GLN – glutamine
HK-ASE – hexokinase
ILE – isoleucine
JWS – Silicon Cell project of Olivier & Snoep[37]
KIVAL – a-ketoisovalerate
LAC – lactate
LALA – L-alanine
MAL – malate
MET – methionine
METsynth – methionine synthesis
M-M – Michaelis-Menten
MMA – the adaptive random optimization algorithm of Maria[51]

mRNA – messenger ribonucleic acid
mTRM – modified Termonia and Ross[30] model
MUR – mureine
MURsynth – mureine synthesis
NAD(P)H – nicotinamide adenine dinucleotide (phosphate) reduced
OAA – oxaloacetate
P – Phosphoric acid
PDH – pyruvate dehydrogenase
PEP – phosphoenolpyruvate
PEPCXYLASE – PEP carboxylase
PFK-ASE – phosphofructokinase
PG1 – glucose-6-phosphate isomerase
PGDH – 6-phosphogluconate dehydrogenase
PGK – phosphoglycerate kinase
PGLUMU – phosphoglycerate mutase
PGM – phosphoglucomutase
PK-ASE – pyruvate kinase
PPP – pentose-phosphate pathway
PTS – phosphotransferase, or phosphoenolpyruvate: glucose phosphotransferase system
PYR – pyruvate
QSS – quasi-steady-state
RIB5P – ribose-5-phosphate
RIBU5P – ribulose-5-phosphate
R5PI – ribose-phosphate isomerase
RPPK – ribose-phosphate pyrophosphokinase
RU5P – ribulose-phosphate epimerase
SED7P – sedoheptulose-7-phosphate
SUCC – succinate
SYNTH1,2 – synthesis 1,2
TA – transaldolase
TCA – tricarboxylic acid cycle
TF – gene expression transcription factors
TKA – transketolase, reaction a
TKB – transketolase, reaction b
TIS – triosephosphate isomerase
TRP – tryptophan
TRPsynth – tryptophan synthesis
XYL5P– xylulose-5-phosphate
[.] – concentration

References

1. *Styczynski, M. P., Stephanopoulos, G.*, Overview of computational methods for the inference of gene regulatory networks, Computers & Chemical Engineering **29** (2005) 519. http://dx.doi.org/10.1016/j.compchemeng.2004.08.029 (2007)
2. *Heinemann, M., Panke, S.,* Synthetic Biology – putting engineering into biology, Bioinformatics **22** (2006) 2790. http://dx.doi.org/10.1093/bioinformatics/btl469 (2007)
3. *Hempel, D. C.,* Development of biotechnological processes by integrating genetic and engineering methods, Engineering in Life Sciences **6** (2006) 443. http://dx.doi.org/10.1002/elsc.200620149 (2008)
4. *Kobayashi, H., Kaern, M., Araki, M., Chung, K., Gardner, T. S., Cantor, C. R., Collins, J. J.,* Programmable cells: Interfacing natural and engineered gene networks, Proceedings of the National Academy of Sciences of the USA **101** (2004) 8414. http://dx.doi.org/10.1073/pnas.0402940101 (2005)
5. *Alon, U.* An introduction to systems biology. Design principles of biological circuits, Chapman & Hall / CRC, Boca Raton, 2007, pp 233–239.
6. *Kholodenko, B. N., Kiyatkin, A., Bruggeman, F. J., Sontag, E., Westerhoff, H. V., Hoek, J. B.,* Untangling the wires: A strategy to trace functional interactions in signalling and gene networks, Proceedings of the National Academy of Sciences of the USA **99** (2002) 12841. http://dx.doi.org/10.1073/pnas.192442699 (2005)
7. *Maria, G.,* Modular-based modelling of protein synthesis regulation, Chemical and Biochemical Engineering Quarterly **19** (2005) 213.
8. *Maria, G,* Application of lumping analysis in modelling the living systems – A trade-off between simplicity and model quality, Chemical and Biochemical Engineering Quarterly **20** (2006) 353.
9. *Maria, G.,* Modelling bistable genetic regulatory circuits under variable volume framework, Chemical and Biochemical Engineering Quarterly **21** (2007) 417.
10. *Maria, G.,* Building-up lumped models for a bistable genetic regulatory circuit under whole-cell modelling framework, Asia-Pacific Journal of Chemical Engineering **4** (2009) 916.
11. *Zak, D. E., Vadigepalli, R., Gonye, G. E., Doyle III, F. J., Schwaber, J. S., Ogunnaike, B. A.,* Unconventional systems analysis problems in molecular biology: A case study in gene regulatory network modelling, Computers & Chemical Engineering **29** (2005) 547. http://dx.doi.org/10.1016/j.compchemeng.2004.08.016 (2006)
12. *Maria, G.,* Relations between apparent and intrinsic kinetics of programmable drug release in human plasma, Chemical Engineering Science **60** (2005) 1709. http://dx.doi.org/10.1016/j.ces.2004.11.009 (2004)
13. *Maria, G.,* A review of algorithms and trends in kinetic model identification for chemical and biochemical systems, Chemical and Biochemical Engineering Quarterly **18** (2004) 195.
14. *Degenring, D., Froemel, C., Dikta, G., Takors, R.*, Sensitivity analysis for the reduction of complex metabolism models, Journal of Process Control **14** (2004) 729. http://dx.doi.org/10.1016/j.jprocont.2003.12.008 (2005)
15. *Costa, R. S., Rocha, I., Ferreira, E. C.,* Model reduction based on dynamic sensitivity analysis: A systems biology case of study, PhD grant report, University of Minho, Braga (Portugal), 2008. http://repositorium.sdum.uminho.pt/bitstream/1822/8421/1/Abstract_Reducit%5B1%5D.pdf (2009)
16. *Chassagnole, C., Noisommit-Rizzi, N., Schmid, J. W., Mauch, K., Reuss, M.,* Dynamic modeling of the central carbon metabolism of Escherichia coli, Biotechnology and Bioengineering **79** (2002) 53. http://dx.doi.org/10.1002/bit.10288 (2002)
17. *He, F., Zeng, A. P.,* In search of functional association from time-series microarray data based on the change trend and level of gene expression, BMC Bioinformatics **7** (2006) 69. http://dx.doi.org/10.1186/1471–2105–7-69 (2007)
18. *He, F., Balling, R., Zeng, A. P.,* Reverse engineering and verification of gene networks: principles, assumptions, and limitations of present methods and future perspectives, Journal of Biotechnology **144** (2009) 190. http://dx.doi.org/10.1016/j.jbiotec.2009.07.013 (2009)

19. *Schmid, J. W., Mauch, K., Reuss, M., Gilles, E. D., Kremling, A.,* Metabolic design based on a coupled gene expression-metabolic network model oftryptophan production in Escherichia coli, Metabolic Engineering **6** (2004) 364. http://dx.doi.org/10.1016/j.ymben.2004.06.003 (2007)
20. *Rodriguez-Prados, J. C., Atauri, P., Maury, J., Ortega, F., Portais, J. C., Chassagnole, C., Acerenza, L., Lindley, N. D., Cascante, M.,* In silico strategy to rationally engineer metabolite production: A case study for threonine in Escherichia coli, Biotechnology and Bioengineering **103** (2009) 609. http://dx.doi.org/10.1002/bit.22271 (2009)
21. *Usuda, Y., Nishio, Y., Iwatani, S., Van Dien, S. J., Imaizumi, A., Shimbo, K., Kageyama, N., Iwahata, D., Miyano, H., Matsui, K.*, Dynamic modeling of Escherichia coli metabolic and regulatory systems for amino-acid production, Journal of Biotechnology **147** (2010) 17. http://dx.doi.org/10.1016/j.jbiotec.2010.02.018 (2011)
22. *Kind, S., Becker, J., Wittmann, C.,* Increased lysine production by flux coupling of the tricarboxylic acid cycle and the lysine biosynthetic pathway – Metabolic engineering of the availability of succinyl-CoA in Corynebacterium glutamicum, Metabolic Engineering **15** (2013) 184. http://dx.doi.org/10.1016/j.ymben.2012.07.005 (2013)
23. *Yazdani, S. S., Gonzalez, R.,* Engineering Escherichia coli for the efficient conversion of glycerol to ethanol and co-products, Metabolic Engineering **10** (2008) 340. http://dx.doi.org/10.1016/j.ymben.2008.08.005 (2008)
24. *Wu, W. H., Wang, F. S., Chang, M. S.,* Multi-objective optimization of enzyme manipulations in metabolic networks considering resilience effects, BMC Systems Biology **5** (2011) 145. http://dx.doi.org/10.1186/1752–0509–5-145 (2012)
25. *Maria, G., Xu, Z., Sun, J.,* Investigating alternatives to in-silico find optimal fluxes and theoretical gene knockout strategies for E. coli cell, Chem. Biochem. Eng. Q. **25** (2011) 403.
26. *Zhu, J., Shimizu, K.,* Effect of a single-gene knockout on the metabolic regulation in Escherichia coli for D-lactate production under microaerobic condition, Metabolic Engineering **7** (2005) 104. http://dx.doi.org/10.1016/j.ymben.2004.10.004 (2010)
27. *Kern, A., Tilley, E., Hunter, I. S., Legisa, M., Glieder, A.*, Engineering primary metabolic pathways of industrial micro-organisms, Journal of Biotechnology **129** (2007) 6. http://dx.doi.org/10.1016/j.jbiotec.2006.11.021 (2012)
28. *Kadir, T. A. A., Mannan, A. A., Kierzek, A. M., McFadden, J., Shimizu, K.,* Modeling and simulation of the main metabolism in Escherichia coli and its several single-gene knockout mutants with experimental verification, Microbial Cell Factories **9** (2010) 88. http://dx.doi.org/10.1186/1475–2859–9-88 (2010)
29. *Selkov, E. E.,* Self-oscillations in glycolysis. 1. A simple kinetic model, European Journal of Biochemistry **4** (1968) 79. http://dx.doi.org/10.1111/j.1432–1033.1968.tb00175.x (2007)
30. *Termonia, Y., Ross, J.*, Oscillations and control features in glycolysis: Numerical analysis of a comprehensive model, Proceedings of the National Academy of Sciences of the USA **78** (1981) 2952. http://dx.doi.org/10.1073/pnas.78.5.2952 (1998)
31. *Termonia, Y., Ross, J.*, Oscillations and control features in glycolysis: Analysis of resonance effects, Proceedings of the National Academy of Sciences of the USA **78** (1981) 3563. http://dx.doi.org/10.1073/pnas.78.6.3563 (1998)
32. *Hatzimanikatis, V., Wang, L.,* The systems engineering of cellular processes, 16th European Symposium on Computer Aided Process Engineering, and 9th International Symposium on Process Systems Engineering, Marquardt, W. and Pantelides, C. (Eds.), Elsevier, Amsterdam, 2006, pp 71–80.
33. *Bier, M., Teusink, B., Kholodenko, B. N., Westerhoff, H. V.,* Control analysis of glycolytic oscillations, Biophysical Chemistry **62** (1996) 15. http://dx.doi.org/10.1016/S0301–4622(96)02195–3 (2002)
34. *Buchholz, A., Hurlebaus, J., Wandrey, C., Takors, R.,* Metabolomics: quantification of intracellular metabolite dynamics, Biomolecular Engineering **19** (2002) 5. http://dx.doi.org/10.1016/S1389–0344(02)00003–5 (2010)
35. *Westermark, P. O., Lansner, A.,* A model of phosphofructokinase and glycolytic oscillations in the pancreatic beta-cell, Biophysical Journal **85** (2003) 126. http://dx.doi.org/10.1016/S0006–3495(03)74460–9 (2010)
36. *Ceric, S., Kurtanjek, Z.*, Model identification, parameter estimation, and dynamic flux analysis of *E. coli* central metabolism, Chemical and Biochemical Engineering Quarterly **20** (2006) 243.
37. *Olivier, B. G., Snoep, J. L.*, Web-based kinetic modelling using JWS Online, Bioinformatics **20** (2004), 2143. (JWS platform – Online Cellular Systems Modelling, http://jjj.biochem.sun.ac.za/info.html). http://dx.doi.org/10.1093/bioinformatics/bth200 (2013)
38. *Laiterä, M.,* Modelling glycolysis with Cellware, course notes S-114.2500, Helsinki University of Technology, 2006. http://www.lce.hut.fi/teaching/S-114.2500/s2006/Glycellw.pdf
39. *Vance, W., Arkin, A., Ross, J.,* Determination of causal connectivities of species in reaction networks, Proceedings of the National Academy of Sciences of the USA **99** (2002) 5816. http://dx.doi.org/10.1073/pnas.022049699 (2013)
40. *Van Someren, E. P., Wessels, L. F. A., Backer, E., Reinders, M. J. T.,* Multi-criterion optimization for genetic network modelling, Signal Processing **83** (2003) 763. http://dx.doi.org/10.1016/S0165–1684(02)00473–5 (2013)
41. *Bussemaker, H. J., Foat, B. C., Ward, L. D.,* Predictive modeling of genome-wide mRNA expression: From modules to molecules, Annual Review of Biophysics and Biomolecular Structure **36** (2007) 329. http://dx.doi.org/10.1146/annurev.biophys.36.040306.132725 (2008)
42. *Ma, H. W., Zhao, X. M., Yuan, Y. J., Zeng, A. P.*, Decomposition of metabolic network into functional modules based on the global connectivity structure of reaction graph, Bioinformatics **20** (2004) 1870. http://dx.doi.org/10.1093/bioinformatics/bth167 (2004)
43. *Maria, G., Luta, I.*, Structured cell simulator coupled with a fluidized bed bioreactor model to predict the adaptive mercury uptake by E. coli cells, Computers & Chemical Engineering **58** (2013) 98. http://dx.doi.org/10.1016/j.compchemeng.2013.06.004 (2013)
44. *Karp, P., Riley, M., Paley, S., Pellegrini-Toole, A., Krummenacker, M.,* EcoCyc: Electronic encyclopedia of E. coli genes and metabolism, Nucleic Acids Research **27** (1999) 55. http://dx.doi.org/10.1093/nar/27.1.55 (2013)
45. *Schaefer, U., Boos, W., Takors, R., Weuster-Botz, D.,* Automated sampling device for monitoring intracellular metabolite dynamics, Analytical Biochemistry **270** (1999) 88. http://dx.doi.org/10.1006/abio.1999.4048 (2013)
46. *Visser, D., Schmid, J. W., Mauch, K., Reuss, M., Heijnen, J. J.*, Optimal re-design of primarymetabolism in Escherichia coli using linlog kinetics, Metabolic Engineering **6** (2004) 378. http://dx.doi.org/10.1016/j.ymben.2004.07.001 (2004)

47. *Lee, F.C., Rangaiah, G. P., Lee, D. Y.*, Modeling and optimization of a multi-product biosynthesis factory for multiple objectives, Metabolic Engineering **12** (2010) 251. http://dx.doi.org/10.1016/j.ymben.2009.12.003 (2012)
48. *Franck, U. F.*, Feedback kinetics in physicochemical oscillators, Berichte der Bunsengesellschaft für Physikalische Chemie **84** (1980) 334. http://dx.doi.org/10.1002/bbpc.19800840407 (2010)
49. *Heyland, J., Blank, L. M., Schmid, A.*, Quantification of metabolic limitations during recombinant protein production in Escherichia coli, Journal of Biotechnology **155** (2011) 178. http://dx.doi.org/10.1016/j.jbiotec.2011.06.016 (2013)
50. *Rao, S. S.,* Engineering optimization – Theory and practice, New York, Wiley, 2009, pp 761–771.
51. *Maria, G.,* In: Proceedings of the 22nd IASTED International Conference on Modelling, Identification, and Control, February 10–13, 2003, Innsbruck, Austria. IASTED/ ACTA Press, Anaheim (CA).
52. *Heinrich, R., Schuster, S.,* The regulation of cellular systems, Chapman & Hall, New York, 1996, pp 138–291. http://dx.doi.org/10.1007/978–1-4613–1161–4_5 (2001)
53. *Roeva, O., Pencheva, T., Tzonkov, S., Arndt, M., Hitzmann, B., Kleist, S., Miksch, G., Friehs, K.*, Multiple model approach to modelling of Escherichia coli fed-batch cultivation extracellular production of bacterial phytase, Journal of Biotechnology **10** (2007) 592.
54. *Mathews, C. K., van Holde, K. E., Ahem, K. G.,* Biochemistry, Prentice Hall, New Jersey, 1999.
55. *Lei, F., Jorgensen, S. B.,* Estimation of kinetic parameters in a structured yeast model using regularisation, Journal of Biotechnology **88** (2001) 223. http://dx.doi.org/10.1016/S0168–1656(01)00272–3 (2013)
56. *Degenring, D., Froemel, C., Dikta, G., Takors*, *R.,* Sensitivity analysis for the reduction of complex metabolism models, Journal of Process Control **14** (2004) 729. http://dx.doi.org/10.1016/j.jprocont.2003.12.008 (2013)
57. *Xiu, Z. L., Zeng, A. P., Deckwer, W. D.,* Model analysis concerning the effects of growth rate and intracellular tryptophan level on the stability and dynamics of tryptophan biosynthesis in bacteria, Journal of Biotechnology **58** (1997) 125. http://dx.doi.org/10.1016/S0168–1656(97)00143–0 (1997)
58. *Schmid, J. W., Mauch, K., Reuss, M., Gilles, E. D., Kremling, A.,* Metabolic design based on a coupled gene expression-metabolic network model of tryptophan production in Escherichia coli, Metabolic Engineering **6** (2004) 364. http://dx.doi.org/10.1016/j.ymben.2004.06.003 (2013)